FEACONS III Computer Program for Analysis of Jointed Concrete Pavements

MANG TIA, JAMSHID M. ARMAGHANI, CHUNG-LUNG WU, SHAU LEI, AND KEVIN L. TOYE

A computer program named FEACONS III (Finite Element Analysis of CONcrete Slabs) was developed in response to a need for a suitable analytical model to analyze the behavior of concrete pavements effectively and realistically. The program has been used extensively in the analysis of existing concrete pavements and a test road in Florida. The analytical model and computational procedure used by FEACONS III are described in detail, and the analytical results from the program are compared with actual measured results for a few specific cases. The FEACONS III program was shown to be both versatile and effective in the analysis of concrete pavement response. The modeling of the edge by means of edge stiffness and the joint by means of linear joint stiffness and torsional joint stiffness produced fairly realistic analytical results. It is hoped that this paper can enhance understanding and proper usage of the program and increase the awareness of highway engineers of the importance of the effects of temperature, joint, edge, and subgrade conditions to concrete pavement response.

During the past few years the University of Florida has been working with the Florida Department of Transportation in the testing and evaluation of concrete pavements in Florida. Some of the objectives of this ongoing research work include (*a*) better understanding of the effects of temperature, moisture, joint, edge, and subgrade conditions on pavement behavior and performance; (*b*) determination of causes of failure in existing pavements; and (*c*) development of an effective and convenient procedure for the use of the falling-weight deflectometer in the evaluation of pavement conditions. In the course of this work, a need arose for a suitable analytical model that could be used to analyze the behavior of concrete pavements effectively and realistically. Subsequently, a computer program named FEACONS (Finite Element Analysis of CONcrete Slabs) was developed. FEACONS was written in a structured fashion such that it could be easily modified and enhanced. The present or third version of the program, named FEACONS III, can analyze the response of a concrete pavement system subjected to combinations of concentrated and uniform vertical loads. It can consider the following factors in the analysis:

1. Weight of concrete slabs,
2. Subgrade voids beneath concrete slabs,
3. Effects of joints,
4. Looseness of dowel bars,
5. Effects of edges,
6. Effects of temperature differentials between the top and the bottom of slabs, and
7. Nonlinear subgrade response characteristics.

The output of the program may include the following:

1. Deflections of concrete slabs due to their own weight and temperature effects;
2. Deflections of concrete slabs due to applied loads;
3. Moments, stresses, and principal stresses in concrete slabs; and
4. Maximum deflection, moments, stresses, and principal stresses in concrete slabs.

FEACONS III has been used extensively in the analysis of existing concrete pavements on a test road in Florida, and some of the results were presented at the Annual Meeting of the Transportation Research Board in 1986 (*1*). The purpose of this paper is to describe in full detail the analytical model and the computational procedure used by FEACONS III and to compare the analytical results from the program with actual measured results for a few specific cases. It is hoped that this paper can enhance the understanding and proper usage of the program and increase awareness of highway engineers of the importance of the effects of temperature, joint, edge, and subgrade conditions to concrete pavement performance.

MODELING OF CONCRETE PAVEMENT

A jointed concrete pavement is modeled by a three-slab system as shown in Figure 1. Each concrete slab is modeled as an assemblage of rectangular plate bending elements with three degrees of freedom at each node, namely,

1. Translation in the vertical (z) direction,
2. Rotation about the x-axis, and
3. Rotation about the y-axis.

The finite-element formulation of the rectangular plate bending element, known as the MZC rectangle, was developed

Department of Civil Engineering, University of Florida, Gainesville, Fla. 32611.

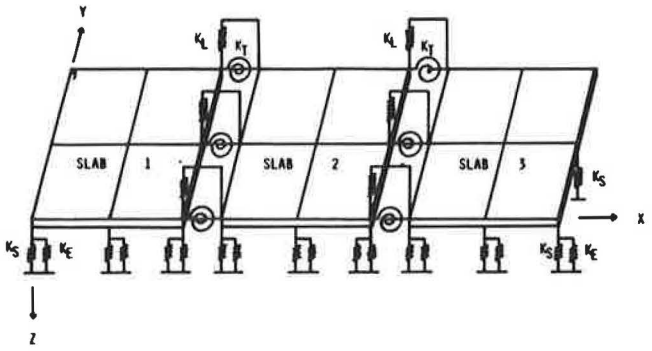

FIGURE 1 Finite-element modeling of a three-slab pavement system.

by Melosh (*2*) and Zienkiewicz and Cheung (*3*). The MZC rectangle has been used widely to model concrete pavement slab behavior in finite-element computer programs such as WESLIQUID and WESLAYER developed by the U.S. Army Corps of Engineers Waterway Experiment Station (*4*), ILLISLAB developed by the University of Illinois (*5*), and the finite-element programs developed by Purdue University (*6*) and the University of Kentucky (*7*). The formulation and characteristics of the MZC rectangular element are presented in the Appendix.

Load transfers across the joints between two adjoining slabs are modeled by shear (or linear) and torsional springs connecting the slabs at the nodes of the elements along the joint. The linear and torsional spring elements and the corresponding stiffness matrix are shown in Figure 2. Looseness of the dowel bars is modeled by a specified slip distance, such that shear and moment stiffnesses become fully effective only when the slip distance is overcome. The effective dowel stiffnesses are modeled as varying linearly with the difference in deflection at the joint, when the difference in deflection is less than the slip distance. The relationship of effective joint stiffnesses and difference in deflection at the joint is shown in Figure 3. Frictional effects at the edges are modeled by shear springs at the nodes along the edges. The subgrade is modeled as a liquid or Winkler foundation by a series of vertical springs at the nodes. Subgrade voids are modeled as initial gaps between the slab and the springs at the specified nodes. A spring stiffness of zero is used when a gap exists. Either a linear or a nonlinear load-deformation relationship for the springs can be specified. For the linear case, the subgrade stiffness remains constant as long as the slab and the subgrade are in contact with one another. For the nonlinear case, a load-deformation relationship of the following form is used:

$$F = Ad + Bd^2 \tag{1}$$

where

F = force/area,
d = deflection, and
A and B = coefficents to be specified in the input.

The subgrade stiffness is thus equal to $A + 2Bd$, which varies with the deflection.

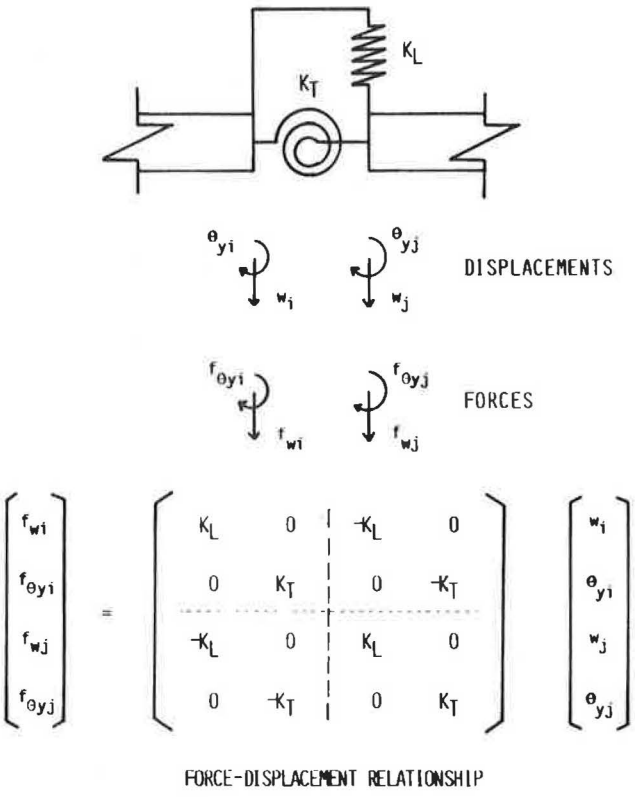

FIGURE 2 Linear and torsional spring elements modeling joint behavior.

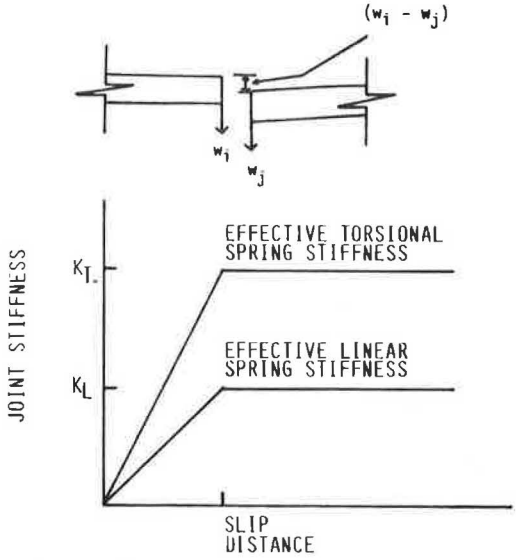

FIGURE 3 Effective joint stiffnesses as functions of the difference in deflection at the joint.

SCHEME OF THE COMPUTER PROGRAM

Figure 4 is a flowchart showing the major computational steps in the FEACONS III program. The program computes the total induced slab deflections in three major steps: First,

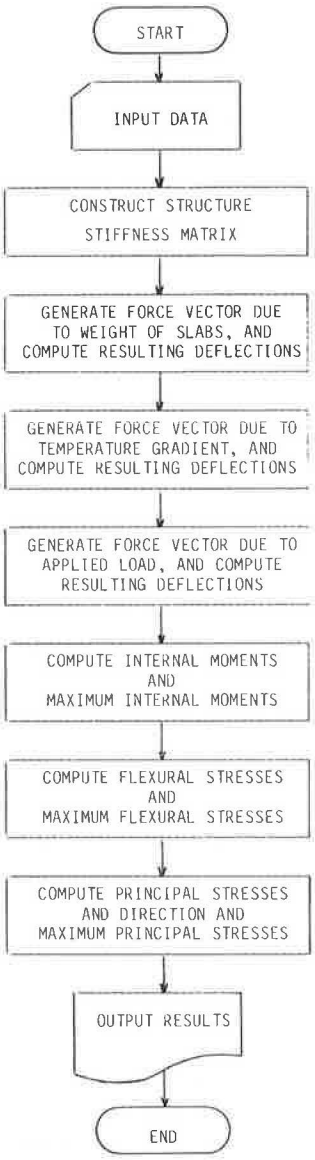

FIGURE 4 Simplified flow chart showing the major steps of FEACONS III.

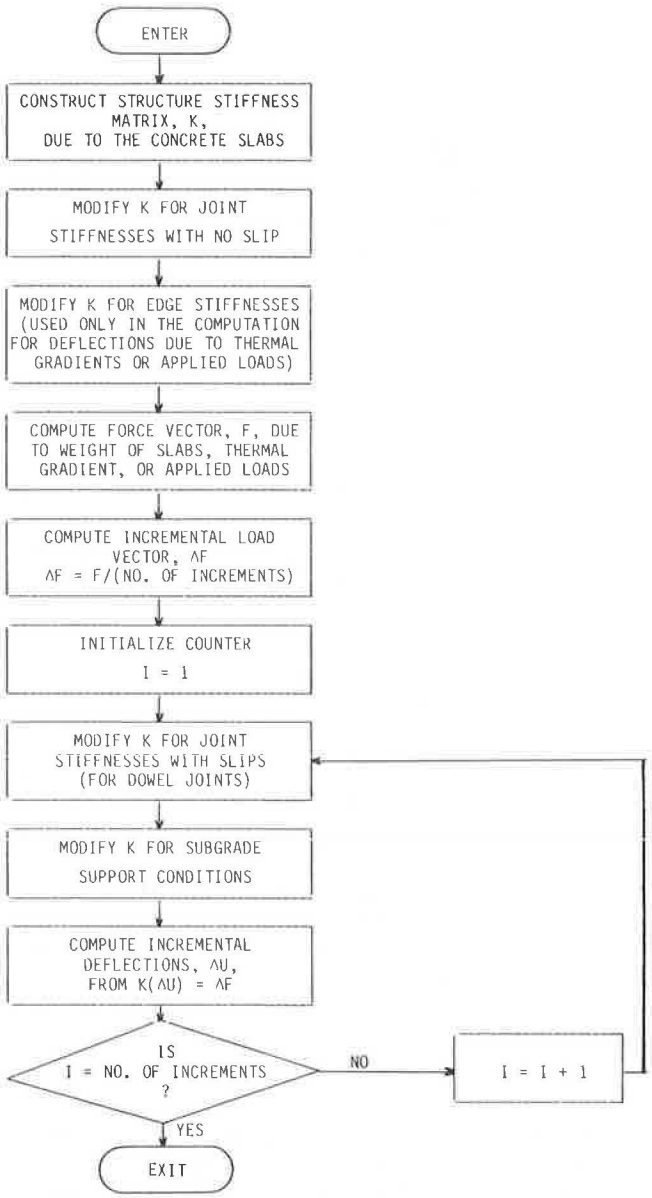

FIGURE 5 Flow chart of scheme for computing slab deflections.

the deflections caused by the weight of the slab are computed. Second, the additional deflections caused by thermal curling are computed. Third, the additional deflections caused by applied loads are computed. The program then computes the internal moment intensities, flexural stresses, and principal stresses in the slab from the final total slab deflections. Computational schemes used in these major steps are described in the following subsections.

Computation of Slab Deflections

Figure 5 is a flowchart that shows the scheme for computing the deflections due to the weight of the slabs, thermal gradients, or applied loads. An incremental computational procedure is used. The force vector (F) due to the weight of the slab, thermal gradients, or applied loads is first computed. The force vector is then divided by the number of increments specified to obtain the incremental load vector (ΔF). The deflections (ΔU) caused by the incremental force vector are computed from the stiffness equation

$$K(\Delta U) = \Delta F \tag{2}$$

where

K = structure stiffness matrix,
ΔU = vector of incremental nodal deflections, and
ΔF = vector of incremental nodal forces.

The structure stiffness matrix (K) is constructed from the stiffness matrices of the plate elements (see Appendix), the stiffness matrices of the joint spring elements, the stiffnesses of the edge springs, and the stiffnesses of the subgrade

springs, according to the finite-element mesh selected and the deflections of the slab at that point. Edge springs are used to model the frictional effects at the edges and thus are used only in the computation for the deflections due to thermal curling and applied loads. After each computation of incremental deflections, K is modified according to the newly deflected positions of the slab. The new K is then used to compute the next set of incremental deflections.

Three numbers, indicating the numbers of increments to be used in the three major computational steps, have to be specified in the program input. In general, the higher the number of increments, the better the accuracy of the results of analysis will be. However, if K does not change throughout a computational step, only an increment of 1 needs to be specified for that computational step. This applies to the case in which the subgrade contact conditions do not change throughout a computational step and no slips are specified at the joints.

The weight of the slabs is modeled as a uniform distributed load. The structure force vector due to the weight of the slabs is constructed from the force vectors of the plate elements due to a uniform distributed load. The explicit expression for the element force vector due to a uniform distributed load is given in Equation A-25 in the Appendix.

The expression for the equivalent nodal forces on a plate element due to a uniform thermal gradient is given in Equation A-27 in the Appendix. These element force vectors are used to generate the structure force vector for the thermal effects.

The structure force vector due to applied loads is constructed from the concentrated nodal forces and the element force vector due to uniform distributed loads.

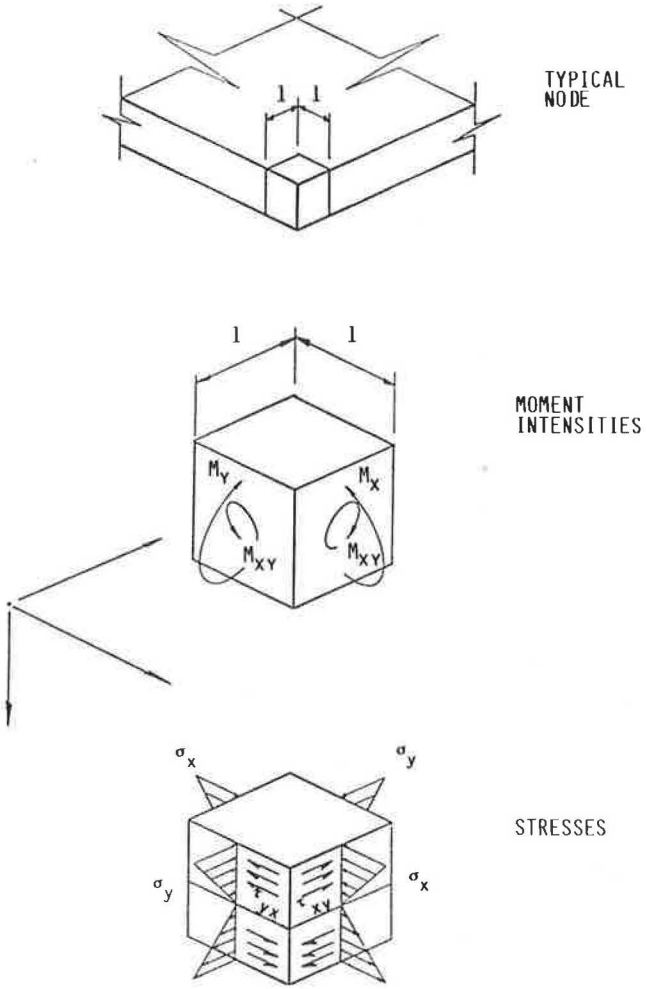

FIGURE 6 Moment intensities and stresses at a node.

Computation of Internal Moment Intensities

The internal moments per unit length at the nodes are calculated from the final nodal deflections. The nodal deflections for each element are first extracted from the final structure deflection vector and then used to compute the internal moment intensities of the element at the nodes. The expression for computing the internal moment intensities is given in Equation A-29 in the Appendix. The moment intensities at each node are the two bending moment intensities (M_x and M_y) and the twisting moment intensity (M_{xy}). M_x is the bending moment intensity due to σ_x, flexural stress in the x-direction. M_y is due to σ_y, flexural stress in the y-direction. M_{xy} is due to τ_{xy}, shearing stress in the xy-direction. The directions of these moment intensities and the corresponding stresses are shown in Figure 6.

Two elements that are incident at the same node may have different moment intensities for that node. This is because only continuity of nodal displacements is required and the moment intensities are dependent on the individual geometry of an element and thus are unique for an individual element. To obtain more representative values of moment intensities for a node, the program calculates the average values of the moment intensities as computed from the adjoining elements and uses them for the computation of stresses.

Computation of Stresses

Flexural and shearing stresses are calculated from the moment intensities using the following equations from classical thin plate theory:

$$\sigma^x = \frac{12z}{t^3} = M_x \tag{3}$$

$$\sigma_y = \frac{12z}{t^3} M_y \tag{4}$$

$$\tau_{xy} = \frac{-12z}{t^3} M_{xy} \tag{5}$$

where t is thickness of the slab and z is distance from the centroid of the slab. The program computes the stresses at the bottom of the slab by setting $z = t/2$ in the equations.

COMPARISON OF FWD MEASUREMENTS WITH ANALYTICAL RESULTS

The FEACONS III program has been used to analyze falling-weight deflectometer (FWD) data obtained from existing concrete pavements. A few examples are presented here to illustrate how the FWD data can be analyzed and how well the analytical results obtained from the FEACONS III program match actual FWD measurements.

Modeling of an FWD Load

The FWD applies an impulse load to the pavement by means of a weight dropped from a specified height onto a circular loading plate, which is usually 30.5 cm (12 in.) in diameter. The FWD load was modeled in the analysis as a static load uniformly distributed over a square area 30.5 × 30.5 cm (12 × 12 in.).

FWD Load at the Center of a Slab

The deflection basin caused by an FWD load applied at the center of a slab can be used to evaluate the subgrade modulus and the concrete modulus of a pavement. A deflection basin is defined here as a profile of maximum induced deflections, which are measured by geophones placed at appropriate positions on the slab. Several prediction equations have been developed by the authors to relate FWD deflections to subgrade modulus. These prediction equations can be used to estimate the subgrade modulus from the FWD deflection data. The FEACONS program can then use these values as the material parameters and compute the expected deflection basin. The computed deflection basin can then be compared with the measured one to determine if the estimated parameter values are reasonable and to adjust these parameter values, if necessary. The details of the interpretation of FWD data will be presented in a follow-up paper. Here, the main purpose is to show how well deflections computed by the FEACONS model match measured deflections.

Example 1 is a 9-kip (40-kN) FWD load at the center of a slab from a test section of I-10 in Jefferson County, Florida. The concrete slab is 12 ft wide, 20 ft long, and 9 in. thick and has doweled joints. The test was run at midnight when the recorded temperature differential between the top and the bottom of the slab is negative. With the temperature lower at the top of the slab, the slab should be curled slightly downward at the center and thus should have full contact with the subgrade at the center. The full contact condition was verified by a plot of FWD load versus deflection at the center of the load that indicated a linear load-deflection relationship. The elastic modulus of the concrete was determined to be 4,076 ksi (28.08 GPa) from core samples taken from the test slab and tested in the laboratory. The subgrade modulus was determined to be 221 pci (60.01 MN/m^3) by the following regression equation:

$$\log_{10}K_s = 3.2507 - 1.8966 \log_{10}D_o \quad (6)$$

where K_s is subgrade modulus (in kci) and D_o is deflection (in μm) at the center of a 9-kip FWD load applied at the center of the slab.

This regression equation is applicable for a concrete slab with a thickness of 9 in. (23 cm) and an elastic modulus of 4,000 ksi (28 GPa) and is an example of the regression equations developed in this study.

The determined values of concrete modulus and subgrade modulus were used as input parameters in the FEACONS III program, and the deflection basin caused by a 9-kip (40-kN) FWD load at the center of the slab was computed. Figure 7 shows the comparison of the measured deflection basin along the longitudinal centerline with the deflection basin computed by the FEACONS III program. It can be noted that the computed deflection basin matches the measured one fairly well.

For this loading condition, results of analysis indicated that edge stiffness (K_E) and joint stiffness (K_L and K_T) had negligible effects because the edges and joints were far from the FWD load.

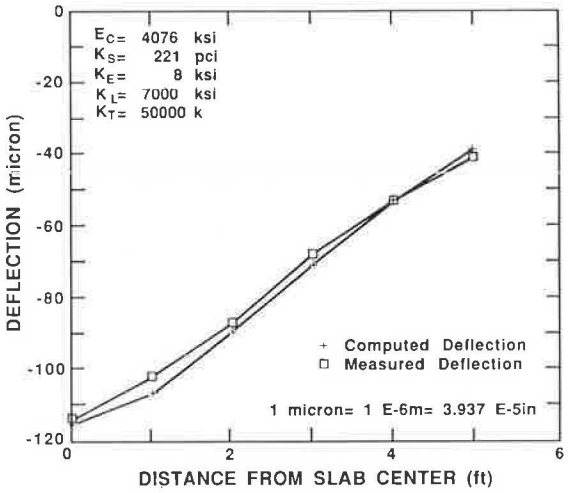

FIGURE 7 Deflection basin along longitudinal centerline due to a 9-kip FWD load at the center of the slab.

FWD Load at the Edge of a Slab

Example 2 is a 9-kip (40-kN) FWD load at the center of the edge of a slab. The test slab is the same one used in Example 1, and thus the material parameters are the same. Tests were conducted at midday when the recorded temperature differential is positive. With the temperature higher at the top of the slab, the slab was curled downward at the edges and had full contact with the subgrade at the edges. This full contact condition was verified by the linear load-deflection relationship observed from the FWD data.

Using the same concrete modulus and subgrade modulus used in Example 1, various deflection basins were calculated by varying K_E and compared with the measured one. By this trial-and-error procedure, K_E was determined to be 8 ksi (55 MPa). Figure 8 shows the comparison of the measured deflection basin along the edge with the computed one from

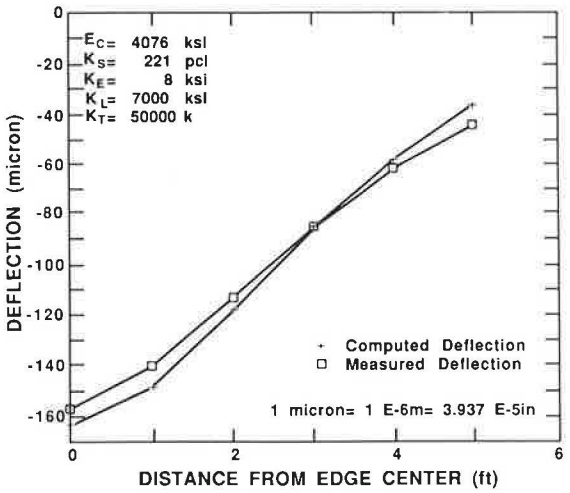

FIGURE 8 Deflection basin along the edge due to a 9-kip FWD load at the edge center.

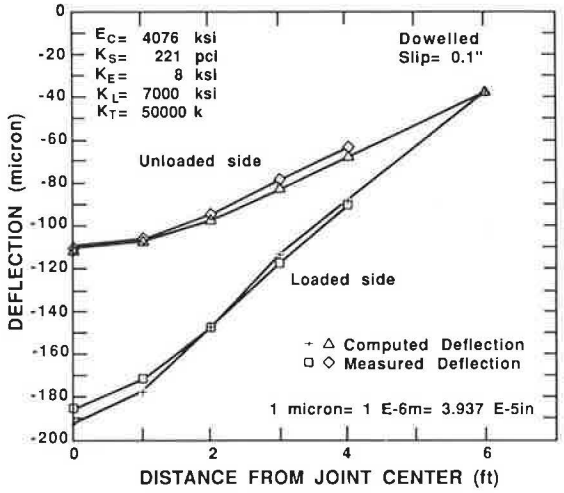

FIGURE 9 Deflection basins along a doweled joint due to a 9-kip FWD load at the center of the joint.

the FEACONS III program. The computed deflection basin matches the measured one fairly well. For this loading condition, analysis results indicated that joint stiffnesses had negligible effects. This was because the joint was far away from the load.

FWD Load at a Doweled Joint

Example 3 is a 9-kip (40-kN) FWD load at the center of a doweled joint. The test slab is the same one used in Examples 1 and 2. Tests were conducted at midday when the slab was curled downward at the edges and joints. It was found that, when the looseness in the dowel bars was modeled with a slip of 0.1 in. (2.54 mm), the computed deflection basin matched the measured one fairly well. Figure 9 shows the comparison of the computed deflection basins and the measured ones along the loaded and the unloaded sides of the doweled joint.

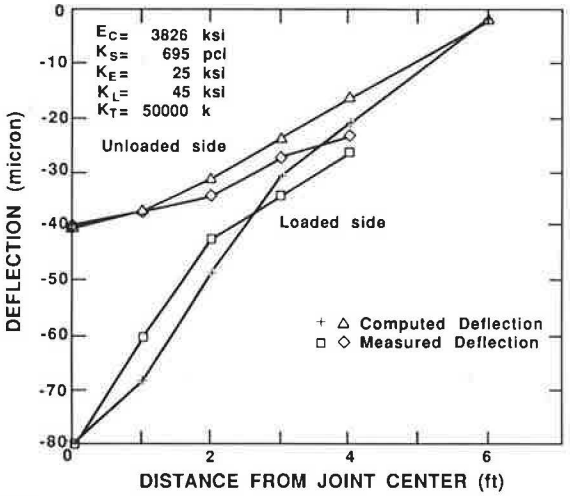

FIGURE 10 Deflection basins along an undoweled joint due to a 9-kip FWD load at the center of the joint.

FWD Load at an Undoweled Joint

Example 4 is a 9-kip (40-kN) FWD load at the center of an undoweled joint. The test was run on a pavement slab on I-10 in Jefferson County, Florida, at midday when the slab was curled downward at the joints and edges. It was found that, by using a linear stiffness of 45 ksi (310 MPa) and a torsional stiffness of 50,000 kips (222.5 MN), a good match between the computed deflection basin and the measured one was achieved. Figure 10 shows the comparison of the computed and measured deflections along the loaded and the unloaded sides of the undoweled joint. Comparison of the performance of the doweled joint and the undoweled joint (Figures 9 and 10) indicates that a doweled joint may not provide a better load transfer mechanism than an undoweled joint, especially when there is excessive looseness in the dowel bars. For this comparison, the deflections at the doweled joint were actually much higher than those at the undoweled joint. This was partly because the subgrade stiffness of the doweled slab was much lower than that of the undoweled slab and partly because there was excessive slip in the doweled joint.

FWD Load at a Doweled Joint with Voids

Example 5 is a 9-kip (40-kN) FWD load at the center of a doweled joint with appreciable voids under the joint. The test was run on a pavement slab on I-10 in Walton County, Florida, at midday when the recorded temperature plots showed that the temperature was higher at the top of the slab. In this case, it was found that a good match between the computed deflections and the measured deflections was achieved by modeling the joint as having a strip of subgrade voids, 12 in. (30 cm) wide and 0.01 in. (0.254 mm) deep, along the entire joint. Figure 11 shows these computed and measured deflection basins along the loaded and the unloaded sides of the joint. In this case, the induced deflections on both sides of the joint were high.

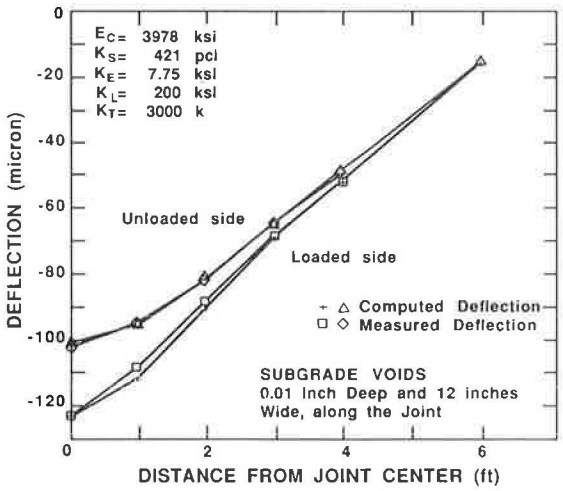

FIGURE 11 Deflection basins along a doweled joint with voids underneath due to a 9-kip FWD load at the center of the joint.

CONCLUSIONS

The analytical model and the computational scheme used by the FEACONS III program for analysis of concrete pavements have been presented in this paper. The computer model used by the FEACONS III program has been shown to be both versatile and effective in the analysis of concrete pavement response.

It has been demonstrated that the edge, joint, and subgrade conditions need to be properly modeled in the analysis. Modeling edge and joint behavior by means of edge stiffness (K_E), linear joint stiffness (K_L), and torsional joint stiffness (K_T) and modeling the subgrade as a Winkler foundation, as used by the FEACONS III program, produced fairly realistic analytical results. The program can be used to estimate pavement parameters (such as subgrade modulus, elastic modulus of concrete, and joint and edge stiffnesses) and to compute the critical induced deflections and stresses caused by a combination of traffic loads and thermal conditions.

ACKNOWLEDGMENTS

The first and second versions of the FEACONS program were developed by K. L. Toye and S. Lei, the fifth and fourth authors of this paper, as their master's theses. The examples presented in the paper were obtained from the results of the project Field Evaluation of Rigid Pavements for the Development of a Rigid Pavement Design System, sponsored by the Florida Department of Transportation. The technical advice and suggestions of B. E. Ruth, L. L. Smith, and T. J. Larsen about the development of the program are gratefully acknowledged. The invaluable technical support and cooperation of C. R. Davis, G. M. Padgett, and J. A. Hughes are greatly appreciated.

APPENDIX: FINITE-ELEMENT FORMULATION OF THE MZC RECTANGLE

Assumptions

The finite-element formulation of the MZC rectangular plate bending element as developed by Melosh (*2*) and Zienkiewicz and Cheung (*3*) is presented in this section. The formulation is based on classical thin plate theory that assumes that (*a*) the thickness of the plate is small compared with its length and width, (*b*) the lateral bending displacements are small compared with the thickness of the plate, and (*c*) normals to the neutral surface remain straight and normal during deformation.

Normal Displacements and Forces

A rectangular plate element is shown in Figure A-1. The three independent displacements at each node are (*a*) lateral deflection (w), (*b*) rotation about the x-axis (Θ_x), and (*c*) rotation about the y-axis (Θ_y). The two rotations (Θ_x and Θ_y) are related to w by the following equations:

$$\Theta_x = -\frac{\partial w}{\partial y} \tag{A-1}$$

$$\Theta_y = \frac{\partial w}{\partial x} \tag{A-2}$$

The three displacements at node i can be denoted as

$$u_i = \begin{bmatrix} w_i \\ \Theta_{xi} \\ \Theta_{yi} \end{bmatrix} \tag{A-3}$$

The 12 nodal displacements of the element can be denoted as

$$u^e = \begin{bmatrix} u_i \\ u_j \\ u_k \\ u_l \end{bmatrix} \tag{A-4}$$

The corresponding forces at each node are (*a*) the downward force (f_w), (*b*) the moment in the x-direction ($f_{\Theta x}$), and (*c*) the moment in the y-direction ($f_{\Theta y}$). The forces at node i are denoted as

$$f_i = \begin{bmatrix} f_w \\ f_{\Theta x} \\ f_{\Theta y} \end{bmatrix} \tag{A-5}$$

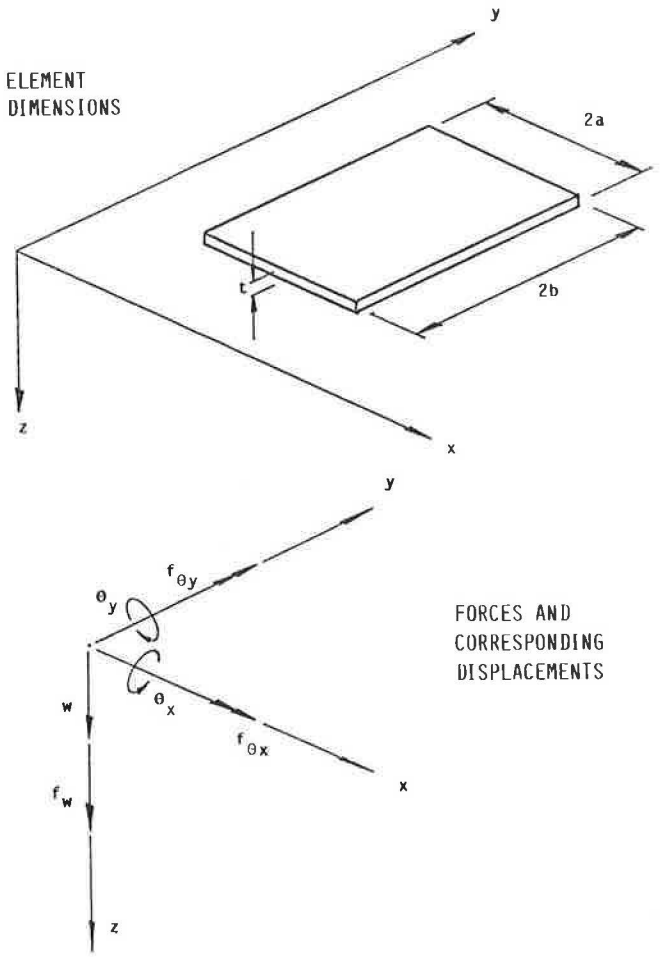

FIGURE A-1 Rectangular plate element.

The 12 nodal forces of the element are denoted as

$$f^e = \begin{bmatrix} f_i \\ f_j \\ f_k \\ f_l \end{bmatrix} \tag{A-6}$$

The displacement function (w) is represented by a polynomial in terms of x and y as

$$\begin{aligned} w = {} & A_1 + A_2x + A_3y + A_4x^2 + A_5xy + A_6y^2 \\ & + A_7x^3 + A_8x^2y + A_9xy^2 + A_{10}y^3 + A_{11}x^3y \\ & + A_{12}xy^3 \end{aligned} \tag{A-7}$$

By investigating this polynomial, it can be seen that along any boundary line, where either x or y is constant, w will vary as a cubic function. Because a cubic function is uniquely defined by four constants, the two end values of slopes and displacements at the two ends will define the displacement along this boundary line uniquely. Because such end values are common to adjacent elements, continuity of w will be imposed all along any interface.

The displacements at node i can now be expressed in terms of x and y coordinates as

$$u_i = \begin{bmatrix} w_i \\ \Theta_{xi} \\ \Theta_{yi} \end{bmatrix} = \begin{bmatrix} w_i \\ \left(-\dfrac{\partial w}{\partial y}\right)_i \\ \left(\dfrac{\partial w}{\partial x}\right)_i \end{bmatrix} = \begin{bmatrix} A_1 + A_2x_i + A_3y_i + A_4x_i^2 + \cdots \\ -A_3 + A_5x_i + 2A_6y_i + A_8x_i^2 + \cdots \\ A_2 + 2A_4x_i + A_5y_i + 3A_7x_i^2 + \cdots \end{bmatrix} \tag{A-8}$$

The 12 nodal displacements of each element can be expressed as

$$u^e = CA \tag{A-9}$$

where C is a 12×12 matrix in terms of the coordinates of the nodes and A is a column matrix of the constants.

Thus the constants A can be expressed as

$$A = C^{-1}u^e \tag{A-10}$$

Curvatures and Internal Moments

The curvatures and twists at any point of the plate can be expressed as

$$\chi = \begin{bmatrix} -\dfrac{\partial^2 w}{\partial x^2} \\ -\dfrac{\partial^2 w}{\partial y^2} \\ 2\dfrac{\partial^2 w}{\partial x \partial y} \end{bmatrix} = \begin{bmatrix} -2A_4 - 6A_7x - 2A_8y - 6A_{11}xy \\ -2A_6 - 2A_9x - 6A_{10}y - 6A_{12}xy \\ 2A_5 + 4A_8x + 4A_9y + 6A_{11}x^2 + 6A_{12}y^2 \end{bmatrix} \tag{A-11}$$

or

$$\chi = BA = BC^{-1}u^e \tag{A-12}$$

where B is a 3×12 matrix in terms of the x- and y-coordinates.

The internal moment intensities (moments per unit length) are related to the curvatures by

$$M = \begin{bmatrix} M_x \\ M_y \\ M_{xy} \end{bmatrix} = D(\chi - \chi_T) \tag{A-13}$$

where

$D = \dfrac{Et^3}{12(1-\nu^2)} \begin{bmatrix} 1 & \nu & 0 \\ \nu & 1 & 0 \\ 0 & 0 & 12(1-\nu) \end{bmatrix}$ for an isotropic material,

E = elastic modulus,

ν = Poisson's ratio,

t = thickness of plate, and

χ_T = curvature changes occurring in an unrestrained element due to temperature alone.

Internal and External Virtual Works

By the principle of virtual work,

$$\delta U_e = \delta W_e \tag{A-14}$$

where δU_e is the virtual internal work (strain energy) and δW_e is the virtual external work on the element caused by a set of virtual nodal displacements (δu^e).

The virtual external work due to the concentrated nodal loads f_c is

$$\delta W_{ec} = (\delta u^e)^T f_c \tag{A-15}$$

The virtual external work due to the distributed load q is

$$\delta W_{eD} = \iint (\delta w)^T q \, dx \, dy \tag{A-16}$$

Equation A-7 can be rewritten as

$$\begin{aligned} w &= \{1,x,y,x^2,xy,y^2,x^3,x^2y,xy^2,y^3,x^3y,xy^3\}A \\ &= PA \end{aligned} \tag{A-17}$$

From Equations A-10 and A-17,

$$\begin{aligned} \delta w &= \delta(LC^{-1} u^e) \\ &= PC^{-1} \delta u^e \end{aligned} \tag{A-18}$$

Substituting Equation A-18 into A-16 gives

$$\begin{aligned} \delta W_{eD} &= \iint (PC^{-1}\delta u^e)^T q \, dx \, dy \\ &= (\delta u^e)^T (C^{-1})^T \iint P^T q \, dx \, dy \end{aligned} \tag{A-19}$$

The total virtual internal work can be expressed as

$$\delta U_e = \iint (\delta \chi)^T M \, dx \, dy \tag{A-20}$$

By using Equation A-12,

$$\delta \chi = BC^{-1}\delta u^e \tag{A-21}$$

Substituting Equations A-13 and A-21 into A-20 gives

$$\begin{aligned} \delta U_e &= \iint (BC^{-1}\delta u^e)^T D(\chi - \chi_T) \, dx \, dy \\ &= \iint (BC^{-1}\delta u^e)^T D(BC^{-1}u^e - \chi_T) \, dx \, dy \\ & (\delta u^e)^T [(C^{-1})^T \{\iint B^T DB \, dx \, dy\} C^{-1} u^e \\ & - (C^{-1})^T \iint BD\chi_T \, dx \, dy] \end{aligned} \tag{A-22}$$

Force-Displacement Relationship

Substituting the expressions for virtual external work and virtual internal work into the virtual work Equation A-14,

$$\begin{aligned} & \delta U_e = \delta W_{ec} + \delta W_{eD} \\ & \rightarrow (\delta u^e)^T [(C^{-1}) \{ \iint B^T DB \, dx \, dy \} C^{-1} u^e - (C^{-1})^T \iint BD\chi_T dx \, dy] \\ & \quad = (\delta u^e)^T f^c + (\delta u^e)^T (C^{-1})^T \iint P^T q \, dx \, dy \\ & \rightarrow (C^{-1})^T \{\iint B^T DB \, dx \, dy\} C^{-1} u^e - (C^{-1})^T \iint BD\chi_T dx \, dy \\ & \quad = f_c + (C^{-1})^T \iint P^T q \, dx \, dy \\ & \rightarrow ku^e - f_T = f_C + f_D \\ & \rightarrow ku^e = f_C + f_D + f_T \end{aligned} \tag{A-23}$$

where

k = $(C^{-1})^T (\iint B^T DB \, dx \, dy) C^{-1}$, element stiffness matrix;
f_D = $(C^{-1})^T \iint P^T q \, dx \, dy$, equivalent nodal loads due to distributed loads; and
f_T = $(C^{-1})^T \iint BD\chi_T \, dx \, dy$, equivalent nodal loads due to temperature changes.

Element Stiffness Matrix

The explicit expression for the element stiffness matrix has been evaluated by Zienkiewicz (*8*). For an isotropic material, it can be expressed as

$$\begin{aligned} k = \frac{Et^3}{720\,ab(1-\nu^2)} [L] \Big(& [SK]_1 + [SK]_2 + \nu[SK]_3 \\ & + \frac{(1-\nu)}{2} [SK]_4 \Big) [L] \end{aligned} \tag{A-24}$$

where

$2a$ = length of the element,
$2b$ = width of the element,
$[L]$ = $\begin{bmatrix} J & & & \\ & J & & \\ & & J & \\ & & & J \end{bmatrix}$ and $J = \begin{bmatrix} 1 & 0 & 0 \\ 0 & 2b & 0 \\ 0 & 0 & 2a \end{bmatrix}$,
E = elastic modulus,
ν = Poisson's ratio,
t = thickness of plate, and
$[SK]_1$, $[SK]_2$, $[SK]_3$, and $[SK]_4$ are as given in Table A-1.

Equivalent Nodal Loads Due to Uniform Distributed Loads

When a uniform distributed load of q acts over an element, the equivalent nodal loads can be calculated to be

$$fD = (C^{-1})^T \iint P^T q \, dx \, dy = 4\,abq \begin{bmatrix} 1/4 \\ -b/12 \\ a/12 \\ 1/4 \\ b/12 \\ a/12 \\ 1/4 \\ -b/12 \\ -a/12 \\ 1/4 \\ b/12 \\ -a/12 \end{bmatrix} \tag{A-25}$$

TABLE A-1 COMPONENT MATRICES OF ELEMENT STIFFNESS MATRIX

$[SK]_1 = p^{-2}$

$p^{-2} = \frac{b^2}{a^2}$

60											
0	0										
30	0	20									
30	0	15	60								
0	0	0	0	0							
15	0	10	30	0	20						
-60	0	-30	-30	0	-15	60					
0	0	0	0	0	0	0	0				
30	0	10	15	0	5	-30	0	20			
-30	0	-15	-60	0	-30	30	0	-15	60		
0	0	0	0	0	0	0	0	0	0	0	
15	0	5	30	0	10	-15	0	10	-30	0	20

Symmetrical

$[SK]_2 = p^2$

$p^2 = \frac{a^2}{b^2}$

60											
-30	20										
0	0	0									
-60	30	0	60								
-30	10	0	30	20							
0	0	0	0	0	0						
30	-15	0	-30	-15	0	60					
-15	10	0	15	5	0	-30	20				
0	0	0	0	0	0	0	0	0			
-30	15	0	30	15	0	-60	30	0	60		
-15	5	0	15	10	0	-30	10	0	30	20	
0	0	0	0	0	0	0	0	0	0	0	0

Symmetrical

$[SK]_3 =$

30											
-15	0										
15	-15	0									
-30	0	-15	30								
0	0	0	15	0							
-15	0	0	15	15	0						
-30	15	0	30	0	0	30					
15	0	0	0	0	0	-15	0				
0	0	0	0	0	0	-15	15	0			
30	0	0	-30	-15	0	-30	0	15	30		
0	0	0	-15	0	0	0	0	0	15	0	
0	0	0	0	0	0	15	0	0	-15	-15	0

Symmetrical

$[SK]_4 =$

84											
-6	8										
6	0	8									
-84	6	-6	84								
-6	-2	0	6	8							
-6	0	-8	6	0	8						
-84	6	-6	84	6	6	84					
6	-8	0	-6	2	0	-6	8				
6	0	-2	-6	0	2	-6	0	8			
84	-6	6	-84	-6	-6	-84	6	6	84		
6	2	0	-6	-8	0	-6	-2	0	6	8	
-6	0	2	6	0	-2	6	0	-8	-6	0	8

Symmetrical

Equivalent Nodal Loads Due to Uniform Temperature Gradients

When the temperature varies linearly from the top to the bottom of the plate with a temperature differential of ΔT, the curvatures of the unrestrained plate element will be

$$\chi_T = \begin{bmatrix} -\dfrac{\partial^2 w}{\partial x^2} \\ -\dfrac{\partial^2 w}{\partial y^2} \\ 2\dfrac{\partial^2 w}{\partial x \partial y} \end{bmatrix}_T = \begin{bmatrix} -\dfrac{\alpha \Delta T}{t} \\ -\dfrac{\alpha \Delta T}{t} \\ 0 \end{bmatrix} \quad \text{(A-26)}$$

where

α = coefficient of thermal expansion,
ΔT = (temperature at top) - (temperature at bottom), and
t = thickness of plate element.

The equivalent nodal loads due to this uniform temperature gradient can be evaluated explicitly to be

$$f_T = (C^{-1})^T \iint B D \chi_T \, dx \, dy = \frac{Et^2 \, \alpha \Delta T}{12(1 - \nu)} \begin{bmatrix} 0 \\ a \\ -b \\ 0 \\ -a \\ -b \\ 0 \\ a \\ b \\ 0 \\ -a \\ b \end{bmatrix} \quad \text{(A-27)}$$

Computation of Internal Moments

After the nodal displacements of an element (u^e) have been determined, the internal moments can be calculated by using Equations A-12 and A-13 as

$$M = \begin{bmatrix} M_x \\ M_y \\ M_{xy} \end{bmatrix} = D(\chi - \chi_T)$$

$$= DBC^{-1} u^e - D\chi_T$$
$$= Su^e - D\chi_T \quad \text{(A-28)}$$

TABLE A-2 STRESS MATRIX

$$S = \frac{1}{4ab}$$

$6p^{-1}D_x + 6pD_1$	$-8aD_1$	$8bD_x$	$-6pD_1$	$-4aD_1$	0	$-6p^{-1}D_x$	0	$4bD_x$	0	0	0
$6pD_y + 6p^{-1}D_1$	$-8aD_y$	$8bD_1$	$-6pD_y$	$-4aD_y$	0	$-6p^{-1}D_1$	0	$4bD_1$	0	0	0
$-2D_{xy}$	$4bD_{xy}$	$-4aD_{xy}$	$2D_{xy}$	0	$4aD_{xy}$	$2D_{xy}$	$-4bD_{xy}$	0	$-2D_{xy}$	0	0
$-6pD_1$	$4aD_1$	0	$6p^{-1}D_x + 6pD_1$	$8aD_1$	$8bD_x$	0	0	0	$-6p^{-1}D_x$	0	$4bD_x$
$-6pD_y$	$4aD_y$	0	$6pD_y + 6p^{-1}D_1$	$8aD_y$	$8bD_1$	0	0	0	$-6p^{-1}D_1$	0	$4bD_1$
$-2D_{xy}$	0	$-4aD_{xy}$	$2D_{xy}$	$4bD_{xy}$	$4aD_{xy}$	$2D_{xy}$	0	0	$-2D_{xy}$	$-4bD_{xy}$	0
$-6p^{-1}D_x$	0	$-4bD_x$	0	0	0	$6p^{-1}D_x + 6pD_1$	$-8aD_1$	$-8bD_x$	$-6pD_1$	$-4aD_1$	0
$-6p^{-1}D_1$	0	$-4bD_1$	0	0	0	$6pD_y + 6p^{-1}D_1$	$-8aD_y$	$-8bD_1$	$-6pD_y$	$-4aD_y$	0
$-2D_{xy}$	$4bD_{xy}$	0	$2D_{xy}$	0	0	$2D_{xy}$	$-4bD_{xy}$	$-4aD_{xy}$	$-2D_{xy}$	0	$4aD_{xy}$
0	0	0	$-6p^{-1}D_x$	0	$-4bD_x$	$-6pD_1$	$4aD_1$	0	$6p^{-1}D_x + 6pD_1$	$8aD_1$	$-8bD_x$
0	0	0	$-6p^{-1}D_1$	0	$-4bD_1$	$-6pD_y$	$4aD_y$	0	$6pD_y + 6p^{-1}D_1$	$8aD_y$	$-8bD_1$
$-2D_{xy}$	0	0	$2D_{xy}$	$4bD_{xy}$	0	$2D_{xy}$	0	$-4aD_{xy}$	$-2D_{xy}$	$-4bD_{xy}$	$4aD_{xy}$

$p = a/b$ FOR ISOTROPIC MATERIALS:

$D = D_x = D_y = Et^3/12(1 - \nu^2)$ $\quad D_1 = \nu D$ $\quad D_{xy} = (1 - \nu)D/2$

where S is DBC^{-1}, stress matrix.

The explicit expressions for the stress matrix (S) are given in Table A-2. For uniform temperature gradients, the internal moments can be evaluated to be

$$M = Su^e + \frac{Et^2\alpha\Delta T}{12(1 - \nu)}\begin{bmatrix}1\\1\\0\end{bmatrix} \qquad \text{(A-29)}$$

where ΔT is (top temperature) - (bottom temperature).

REFERENCES

1. J. M. Armaghani, J. M. Lybas, M. Tia, and B. E. Ruth. Concrete Pavement Joint Stiffness Evaluation. In *Transportation Research Record 1099,* TRB, National Research Council, Washington, D.C., 1986, pp. 22-37.
2. R. J. Melosh. Basis of Derivation of Matrices for the Direct Stiffness Method. *AIAA Journal,* Vol. 1, No. 7, July 1963, pp. 1631-1637.
3. O. C. Zienkiewicz and Y. K. Cheung. The Finite Element Method for Analysis of Elastic Isotropic and Orthotropic Slabs. *Proc., Institute of Civil Engineers,* Vol. 28, 1964, pp. 471-488.
4. Y. T. Chou. *Structural Analysis Computer Programs for Rigid Multicomponent Structures with Discontinuities—WESLIQUID and WESLAYER.* Technical Report GL-80. U.S. Army Waterways Experiment Station, Vicksburg, Miss., Sept. 1980.
5. A. Tabatabaie and E. J. Barenberg. Finite Element Analysis of Jointed or Cracked Concrete Pavements. In *Transportation Research Record 671,* TRB, National Research Council, Washington, D.C., 1978, pp. 11-20.
6. J. Larralde and W. F. Chen. Computer Model for Analysis of Rigid Pavements with Fatigue. *Proc., Third International Conference on Concrete Pavement Design and Rehabilitation,* Purdue University, West Lafayette, Ind., April 1985, pp. 537-547.
7. Y. H. Huang. Finite Element Analysis of Concrete Slab and Its Implications for Rigid Pavement Design. In *Highway Research Record 466,* HRB, National Research Council, Washington, D.C., 1973, pp. 55-99.
8. O. C. Zienkiewicz. *The Finite Element Method,* 3d ed. McGraw-Hill Book Company, London, England, 1977.

Publication of this paper sponsored by Committees on Rigid Pavement Design, on Rigid Pavement Construction and Rehabilitation, and on Pavement Rehabilitation.